Quantum Chemical and Free Energy Simulation Analysis of Retinal Conformational Energetics

Jérôme Baudry,[‡] Serge Crouzy,[§] Benoît Roux,[†] and Jeremy C. Smith*,[‡]

Section de Biophysique des Protéines et des Membranes, DBCM, CEA-Saclay, 91191 Gif-sur-Yvette Cedex, France, BMC/DBMS CEA-Grenoble, 38054 Grenoble Cedex 9, France, and Chemistry Department, Université de Montréal, Montréal H3C 3J7, Canada

Received July 2, 1997[⊗]

Ab initio quantum chemical and free energy molecular dynamics calculations are performed to examine energy differences between the *all-trans* and *(13,15)cis* conformers of retinal, *i.e.,* those populated in the dark-adapted state of bacteriorhodopsin. The quantum chemical results are used to derive an empirical force field that is used to calculate an adiabatic potential energy map for rotation about the bonds concerned. The same potential function is used in restrained molecular dynamics free energy calculations, with and without umbrella sampling. The simulation model yields a free energy of the *(13,15)cis* isomer ∼2.1 kcal/mol higher than that of the *all-trans* species.

INTRODUCTION

The retinal molecule (Figure 1) plays an important role in many physiological processes. One of these is the light-driven proton pumping in bacteriorhodopsin (bR), the protein of the purple membrane of the bacterium *Halobacterium salinarium.*[1] Retinal is covalently bonded to Lys 216 in the bR molecule and acts as the chromophore in the bR photocycle. Electron cryomicroscopy has been used to obtain an atomic-resolution three-dimensional structure of bR in which the retinal is in the light-adapted, *all-trans* conformation,[2,3] a state that absorbs at 568 nm. This structure is of sufficient accuracy to be used as the basis for atomic-detail simulations of the system. These simulations can be performed to examine aspects of the structure and to simulate steps along the bR photocycle.[4−10]

In previous work we presented a simulation model of bR_{568}[7] and examined the thermodynamic stability of internal water molecules in the protein.[8−10] In the present paper we examine energetics of retinal conformers that characterize the dark-adapted state. The dark-adapted state absorbs at 558 nm and contains a mixture of two isomers of retinal—*all-trans,* in which all the double bonds of the polyene are in the *trans* conformation, and *C13═C14 cis, C15═N16 syn,* abbreviated here to *(13,15)cis,* in which the dihedral angles C13═C14 and C15═N16 are both *cis*.[11] A variety of experiments, including retinal extraction followed by high-pressure liquid chromatography,[12] ^{13}C nuclear magnetic resonance spectroscopy,[11] and Raman spectroscopy,[13,14] have suggested that under physiological conditions the population ratio of *(13,15)cis* to *all-trans* is between ∼50% and ∼66%. The approximately equal populations of the two forms suggests that the difference in their free energies is less than k_bT (where k_b is Boltzmann's constant and T is the temperature). The population ratio is modified by changes in temperature, pH, amino-acid sequence of bR, pressure, and lipid composition of the membrane.[12−14]

Both the *all-trans* and *(13,15)cis* isomers have their own photocyles, but only that of the *all-trans* isomer leads to proton pumping.[15] In recent MD work a structure was proposed for *(13,15)cis*, its photocycle was simulated,[15] and the dark-adaptation mechanism was examined.[16] Here we use quantum chemical analysis and free energy simulation to examine the relative energies of *all-trans*- and *(13,15)-cis*-retinal. In the first part of the work *ab initio* quantum chemical calculations are performed to probe the conformational energetics of a retinal fragment. The results of these calculations are used to refine an empirical molecular mechanics force field for retinal which is subsequently employed to calculate the free energy difference between the *all-trans* and *(13,15)cis* states, using molecular dynamics with and without umbrella sampling.

METHODS

***Ab Initio* Calculations on Retinal Fragments.** *Ab initio* calculations were performed on the following three molecules, using the GAUSSIAN 90 program[20] with the RHF/6-31G* basis set: (i) NMM3P: *N*-methyl-methyl-3-pentenylidenimine, CH_3-NH═CH-CH═C(CH_3)-CH═CH_2 (Figure 2a), (ii) NMB: (*E*)-*N*-methyl-2-butenylidenimine, CH_3-NH═CH-CH═CH-CH_3, (Figure 2b), and (iii) AMP: amine-l-methyl-3-pentenylidenimine, NH_2═CH-CH═C(CH_3)-CH═CH_2 (Figure 2c). Geometry optimizations were performed on two isomers of the NMB molecule, in which the C_ϵ−N16═C15-C14 dihedral is *trans* (defined as *trans* NMB), or *cis* (defined as *cis* NMB), and on two isomers of the AMP molecule in which the C15−C14═C13−C12 dihedral is *trans* (defined as *trans* AMP) or *cis* (defined as *cis* AMP). The optimizations were performed while constraining the molecules to *C*2 symmetry, in which all the atoms are coplanar except for the two hydrogens in each of the Cϵ and C20 methyl groups.

NMM3P is a protonated Schiff base with a formal charge of +1 and is conjugated over three double bonds. The carbon C13 is methylated, as in retinal. The molecule thus contains eight heavy (non-hydrogen) atoms. NMM3P was built using the optimized fragments of the NMB and AMP molecules. Four conformers of NMM3P were optimized:

† Université de Montréal.
‡ Section de Biophysique des Protéines et des Membranes.
§ BMC/DBMS CEA-Grenoble.
⊗ Abstract published in *Advance ACS Abstracts,* November 1, 1997.

S0095-2338(97)00239-4 CCC: $14.00

all-trans, in which the C_ϵ−N═C15−C14 and C15−C14═C13−C12 dihedrals are both *trans*, and the corresponding *(13,15)cis*, (13*cis* 15*trans*), and (13*trans* 15*cis*) conformers. The geometries of the NMM3P were optimized using the RHF/6-31G* basis set. To evaluate the energy differences between the conformers of NMM3P single point calculations were made with various basis sets and electron correlation up to the MP2 level.

Determination of the Molecular Mechanics Force Field. The determination of an accurate molecular mechanics force field is prerequisite to the subsequent evaluation of reliable thermodynamic energies using simulation methods.

The CHARMM[21] potential energy function was employed in all the molecular mechanics and dynamics calculations and has the following form

$$V = \sum_{bonds} k_b(b - b_0)^2 + \sum_{angles} k_\theta(\theta - \theta_0)^2 + \sum_{1:3} k_u(u - u_0)^2 + \sum_{dihedrals} k_\phi(1 + cos[n\phi - \delta]) + \sum_{impropers} k_\omega(\omega - \omega_0)^2 + \sum_{i,j} 4\epsilon_{ij}\left[\left(\frac{\sigma_{ij}}{r_{ij}}\right)^{12} - \left(\frac{\sigma_{ij}}{r_{ij}}\right)^{6}\right] + \sum_{i,j} \frac{1}{4\pi\epsilon} \frac{q_i q_j}{r_{ij}} \quad (1)$$

The potential energy function includes bonded interactions, comprising bond stretches, bond angle bends and dihedral angle contributions, and nonbonded interactions between pairs (i, j) of atoms. In eq 1, b, u, θ, and ω are the bond lengths, Urey-Bradley 1:3 distances, angles, and improper dihedral angles in any given configuration, and b_0, u_0, θ_0, ω_0 are the reference values for these properties; the associated force constants are k_b, k_u, k_θ, and k_ω. The improper dihedral contributions are used to represent out-of-plane deformations of the sp^2 groups. For the intrinsic dihedral angles ϕ, k_ϕ *is* the force constant, n is the symmetry number of the rotor (*e.g.*, 3 for a methyl group), and δ is the phase angle.

The nonbonded interactions are included between pairs i, j of atoms separated by three or more bonds. They consist of a Lennard-Jones term, with parameters $\epsilon_{i,j}$ and $\sigma_{i,j}$ and a Coulombic electrostatic term between partial charges q_i, q_j. The dielectric constant, $\epsilon = \epsilon_0 \cdot \epsilon_r$ was set to $\epsilon = \epsilon_0$, *i.e.*, $\epsilon_r = 1$. Hydrogen bonds are described by the nonbonded terms in the energy function. In all the calculations long-range electrostatic terms were smoothly brought to zero at a cutoff of 12 Å by multiplication by a cubic switching function between 10 and 12 Å. Pairs of atoms on the same molecule separated by only two bonds may interact *via* a Urey-Bradley term harmonic in the distance between atoms i, j. In previous work[8,9] a force field was developed based on *ab initio* and semiempirical quantum chemistry calculations on an *all-trans* retinal fragment and *all-trans* retinal. In the present work this force field was refined to reproduce the *ab initio* conformational energetics of NMM3P. The final force field parameters are given in refs 9 and 10 together with the modified parameters that are listed in Set A of Table 1.

Automatic Map Refinement Procedure—AMRP. Adiabatic potential energy and MD free energy calculations were performed on the retinal structure bonded to lysine depicted in Figure 1. The potential function was used to derive an adiabatic potential energy map for rotation about the C13═C14 and C15═N16 dihedrals of retinal. The method used—which we call the Automatic Map Refinement Procedure (AMRP)—allows the derivation of a one- or two-dimensional adiabatic energy map. The procedure is explained here for the case of a one-dimensional energy vector representing the energies obtained at N different values of a reaction coordinate, ξ. The program takes as input the list of N structure file names and energies ranked in increasing order of ξ from which a list of neighbors to each structure is calculated. In the case of a periodic ξ, the structures 1 and N are neighbors to each other. The energy refinement involves the following steps:

(1) The program looks for all local minima in the map that have not yet been used as initial structures for refinement (flag unset) and energy minimizes each of their two neighbors—(their only neighbor for minima 1 or N or cases without dihedral periodicity)—from the coordinates of the minima.

(2) After one pass over all minima, the program checks that these minima still have an energy lower than the newly-minimized structures. If such is the case, a flag is set to indicate that these minima have already been used as initial structures for refinement, the next minima are calculated and the loop continues with Step 1. If, on the other hand, a newly-minimized structure, m_1, has an energy lower than the minimum m_0 used to calculate m_1, then the flag on m_0 is unset, m_1 is kept, and the loop continues with step 1. The loop ends when all points in the map have been flagged as minima.

The above procedure can be easily extended to an n-dimensional map by changing the number of neighbors from 2 to 2.n. The method ensures smoothing of the adiabatic map and removal of hysteresis in the case of a periodic ξ. However, the calculations can become quite time-consuming for $n > 2$. Therefore, to limit computer time, the required precision in the comparison of the energies of a minimum and its minimized neighbor should be a function of the system size (0.1 kcal/mol, typically, for more than 1000 atoms). A logfile is written containing all the refinement steps done so that the program can be stopped and restarted easily. The ARMP program is available by e-mail from S.C. at crouzy@bonne.ceng.cea.fr.

Table 1. Dihedral and van der Waals Parameters of the Potential Energy Function, in CHARMM Notation[21] [a]

				k_ϕ (kcal/mol)	n	δ (deg)
		Set A				
X	C13	C14	X	3.15[b]	2	180
C12	C13	C14	C15	0.65	1	0
X	C15	N16	X	3.55[c]	2	180
C14	C15	N16	C_ϵ	0.51	1	180
R_{min} (Å)	E_{min} (*kcal/mol*)					
1.6	−0.11					
		Set B				
X	C13	C14	X	0.3	2	180
C12	C13	C14	C15	0.65	1	0
X	C15	N16	X	0.3	2	180
C14	C15	N16	C_ϵ	0.51	1	180
R_{min} (Å)	E_{min} (*kcal/mol*)					
1.6	−0.11					

[a] Set A: The full parameter set used to obtain the results of Table 5 line b. Set B: Parameters used in MD free energy simulations. "X" means wildcard atom. Four terms contribute to the $n = 2$ dihedrals and one term to the $n = 1$ dihedrals. R_{min} is the van der Waals radius of the "1−4" vicinal sp^2 carbons (i.e., "CR*" Atom Type[9]), and E_{min} is the depth of the corresponding potential energy well. [b] k_ϕ from ref 5. [c] k_ϕ from ref 17.

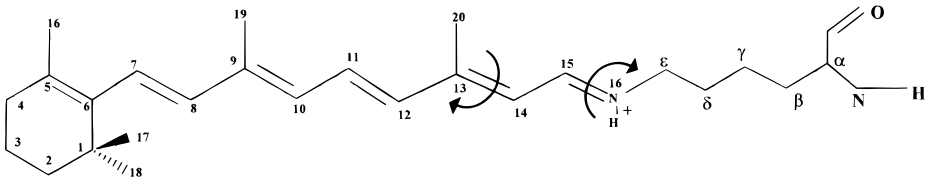

Figure 1. Atom numbering for retinal bonded to lysine. The arrows indicate the isomerized double bonds.

Table 2. Force Constants for Harmonic Restraints (in kcal/mol/Å^2)

atom (a)	C1	C2	C3	C4	C5	C6	C7	C8	Cβ	Cγ	Cδ	N	Cα	C	O
	1.3	0.5	0.1	0.1	0.1	2.4	2.4	2.4	0.5	0.5	0.5	3.4	0.3	2.0	1.8

[a] The last four atoms are on the Lys216 backbone.

Table 3. *Ab Initio* Optimized Bond Lengths (in Å) and Bond Angles and Dihedral Angles (in deg) of NMB, AMP, and NMM3P

	NMB		AMP		NMM3P			
bond	15 t	15 c	13 t	13 c	*all-trans*	13tl5c	13c15t	(13,15)*cis*
C15═N16	1.282	1.285	1.297	1.296	1.290	1.293	1.289	1.292
C14−C15	1.429	1.427	1.406	1.409	1.415	1.413	1.417	1.415
H15−C15	1.076	1.076	1.073	1.073	1.073	1.072	1.074	1.072
H14−C14	1.075	1.073	1.075	1.075	1.076	1.073	1.075	1.072
C13═C14	1.340	1.342	1.367	1.367	1.361	1.364	1.362	1.365
C20−C13	1.490	1.489	1.505	1.505	1.505	1.505	1.506	1.506
H20A−C20	1.081	1.081	1.078	1.080	1.079	1.084	1.080	1.080
H20B−C20	1.086	1.086	1.084	1.085	1.084	1.078	1.084	1.084
H20C−C20	1.086	1.086	1.083	1.084	1.084	1.084	1.084	1.084
C$_\epsilon$−N16	1.466	1.467			1.469	1.466	1.469	1.466
H16−N16	1.003	1.000			1.001	0.996	1.001	0.997
Hϵ3−Cϵ	1.080	1.080			1.081	1.078	1.078	1.081
Hϵ2−Cϵ	1.079	1.080			1.078	1.081	1.081	1.078
Hϵ1−Cϵ	1.080	1.080			1.081	1.081	1.081	1.081
C12−C13			1.461	1.462	1.465	1.464	1.466	1.465
C11═C12			1.330	1.329	1.327	1.328	1.327	1.328
H12−C12			1.075	1.073	1.075	1.075	1.073	1.073
H11A−C11			1.073	1.073	1.074	1.074	1.073	1.073
H11B−C11			1.073	1.074	1.074	1.074	1.074	1.074

	NMB		AMP		NMM3P			
angle	15 t	15 c	13 t	13 c	*all-trans*	13t15c	13c15t	(13,15)*cis*
				Bond Angles				
C14−C15═N16	124.6	125.9	123.6	123.6	123.8	125.0	123.7	125.0
H15−C15═N16	116.4	115.7	115.0	115.0	115.3	114.6	115.2	114.5
H14−C14−C15	118.8	119.90	116.8	116.6	116.6	117.6	116.4	117.4
C13═C14−C15	119.6	119.0	125.4	124.5	124.7	124.1	124.8	124.2
C20−C13═C14	125.2	125.2	124.6	117.7	124.7	124.9	117.9	117.7
H20A−C20−C13	112.3	112.3	114.0	111.5	114.0	109.5	111.4	111.4
H20B−C20−C13	109.5	109.5	109.5	110.2	109.6	114.1	110.2	110.2
H20C−C20−C13	109.5	109.5	109.5	110.2	109.6	109.5	110.2	110.2
C15═N16−Ce	126.1	126.3			124.9	126.4	125.0	126.4
H16−N16═C15	117.8	117.2			118.0	117.1	118.0	117.1
Hϵ3−Cϵ−N16	109.2	109.9			110.1	107.9	108.1	110.2
Hϵ2−Cϵ−N16	109.3	110.0			108.1	110./2	110.1	107.9
Hϵ1−Cϵ−N16	109.2	109.9			110.1	110.2	110.1	110.2
C12−C13═C14			116.9	123.7	117.0	116.9	123.7	123.9
C11═C12−C13			124.7	123.7	124.8	124.8	123.9	123.8
H12−C12−C13			116.2	118.6	116.1	116.1	118.4	118.5
H11A−C11═C12			123.5	123.5	123. 5	123.5	123.4	123.4
H11B−C11═C12			120. 3	120.4	120.4	120. 4	120. 5	120.4
				Dihedral Angles				
Hϵ3−Cϵ−N16−H16	−60.0	119.0			−60.9	180.0	180.0	−60.9
Hϵ2−Cϵ−N16−H16	180.0	−119.0			180.0	60.9	60.9	180.0
Hϵ1−Cϵ−N16−H16	60.0	0.0			60.9	−60.9	−60.9	60.9
H20A−C20−C13═C14	0.0	0.0	0.0	0.0	0.0	121.0	0.0	0.0
H20A−C20−C13═C14	121.5	121.6	−121.0	−120.5	−121.0	0.0	−120.5	−120.5
H20A−C20−C13═C14	−121.5	−121.6	121.0	120.5	121.0	−121.0	120.5	120.5

Free Energy Calculations on Retinal Linked to Lysine. The free energy difference between the *all-trans* and *cis* species was calculated along the "bicycle-pedal" pathway, defined as $\phi_1 = -\phi_2$ where ϕ_1 is the C13═C14 dihedral and ϕ_2 is that of C15═N16. This pathway leads to the smallest change in overall shape of the retinal chain and has been suggested to be the pathway followed by the retinal in bR.[15,16,22,23] The present work does not aim to calculate the

most probable pathway but concentrates specifically on the *all-trans* − *(13,15)cis* energy difference.

The force field 2-fold intrinsic dihedral terms lead to barriers of ∼25 kcal/mol to rotation of each of the double bonds.[5,17] This leads to poor sampling of ϕ_1 and ϕ_2 in MD both with and without umbrella sampling. To circumvent this problem the intrinsic dihedral terms along the reaction coordinate were modified; the terms used are given in Table 1 Set B. These terms were used in the adiabatic and MD calculations, which were therefore all performed with the same force field. Twofold cosine terms have minima located at 0° and ±180°, and therefore their modification does not modify the energies of the *all-trans* and (*13*,15)*cis* isomers.

The starting structure for the MD free energy calculations on this molecule was obtained from ref 3. During the MD calculations harmonic restraints were placed on some atoms of the simulated system, so as to keep the retinal in a similar region of configurational space as in the protein. The harmonic restraints were manually optimized from a series of test MD runs to ensure that the "bicycle pedal" diagonal was adequately sampled in a 1 ns MD simulation without umbrella sampling. The harmonic restraints are listed in Table 2.

Free Energy Calculations. The improved force field was used in MD calculations to evaluate the *all-trans* − *(13,15)cis* free energy difference at 300 K with and without umbrella sampling. We call here "free MD" the MD calculation without umbrella sampling. In the free MD run 10 ps equilibration was followed by a Langevin production step of 16 ns, with an integration timestep of 2 fs, saving the coordinates every 20 steps, with a friction coefficient on the heavy atoms of 5 ps^{-1}. The values of the ϕ_1 and ϕ_2 dihedral angles were computed and saved to disk every 40 fs. For each simulation, a two-dimensional probability histogram was calculated, as a function of ϕ_1 and ϕ_2, in bins of 7°. The relative free energy, ΔA was computed using $\Delta A = -k_bT \ln(\rho_i/\rho_{max})$, where ρ_i is the population of bin number i and ρ_{max} is the population of the most populated bin.

The 16 ns free MD free energy profile was compared with shorter, less-expensive umbrella sampling simulations. The umbrella-sampled distributions were analyzed using the Weighted Histogram Analysis Method (WHAM)[18] that has been extended to more than one degree of freedom.[19] In the present WHAM calculations the same potential energy function was used as for the free MD. The potential of mean force was calculated for ϕ_1 ($= -\phi_2$) varying from +180° to −180° in steps of 30° in the following stages: (i) ϕ_1 and ϕ_2 were restrained to the required values with a force constant of 20 kcal/mol/deg^2. (ii) A 10 ps equilibration run was performed. (iii) Langevin production runs were made with time lengths of 125, 180, and 250 ps. ϕ_1 and ϕ_2 were saved every 40 fs.

The total production time was 1.625 ns for the 125 ps production/window, 2.34 ns for the 180 ps production/window, and 3.25 ns for the 250 ps production/window. The total equilibration time was 130 ps (*i.e.*, 10 ps/window). The potentials of mean force were calculated with bin widths of 7°.

RESULTS AND DISCUSSION

Geometries and Conformational Potential Energy Differences. Table 3 lists the geometries of the RHF/6-31G* *ab initio*-optimized molecules. The bond lengths and angles vary between the *ab initio* conformers by less than 0.01 Å and 2°, respectively, with two exceptions: the AMP bond angles, C20−C13═C14 (which closes by ∼7°, from 124.6° in the 13*trans* conformer to 117.7° in the 13*cis* conformer) and C12−C13═C14 (which opens by a similar amount: 13*trans* = 116.9°, 13*cis* = 123.7°). The internal geometries of the *ab initio*-optimized NMM3P are close to the corresponding values of the *ab initio*-optimized AMP and NMB, though they are not equal. The values of the bond lengths and angles in *ab initio*-optimized NMM3P are generally intermediate between the corresponding length in AMP and NMB.

Ab initio calculations were performed to obtain the energy differences between the conformers of NMM3P as described in Methods. The results are listed in Tables 4 and 5. Table 4 gives the results of single-point calculations of the *(13,15)cis-all-trans* energy difference with various basis sets at the Hartree−Fock level or in the presence of second-order Møller−Plesset (MP2) electron correlation corrections. The single-point calculations were performed on the geometries optimized at the RHF/6-31G* level. All the calculations indicate that the *all-trans* conformer has a slightly lower energy than the *(13,15)cis* species, by ∼0.5 kcal/mol. Increasing the basis set up to the 6-31G** level or adding MP2 corrections do not significantly affect this result. Table 5 gives the RHF/6-31G* geometry-optimized energy difference of the isomers of NMM3P. The *all-trans* and *13trans,15cis* isomers are nearly of the same energy, as are

Table 4. *Ab Initio* Single Point (*13,15)cis-all-trans* Energy Difference (in kcal/mol) Using Geometries Optimized at the RHF/6-31G* Level

RHF				MP2		
4-31G	6-31G	6-31G*	6-31G**	4-31G	6-31G	6-31G*
0.46	0.43	0.65	0.63	0.44	0.41	0.58

Table 5. Relative Energies (kcal/mol) of Isomers of NMM3P

	all-trans	*13 trans,15 cis*	*13 cis,l5 trans*	*(13,15)cis*
(a)[a]	0.00	0.00	0.64	0.65
(b)[b]	0.00	0.03	0.62	0.65

[a] (a): RHF/6-31G* geometry optimization. [b] (b): geometry-optimized molecular mechanics.

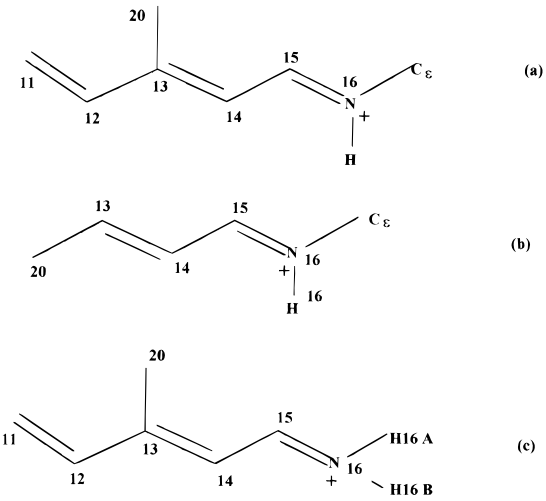

Figure 2. (a) NMM3P, (b) NMB, and (c) AMP.

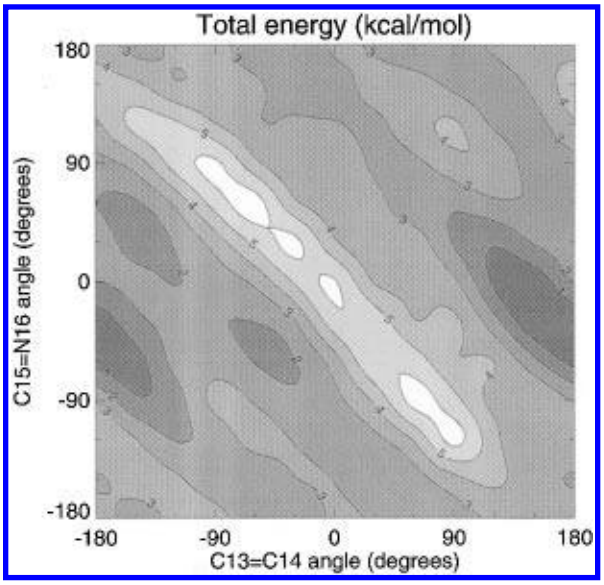

Figure 3. Adiabatic potential energy map for retinal molecule in Figure 1, calculated with the ARMP method. The bicycle pedal pathway is the diagonal from (180,−180) to (0,0).

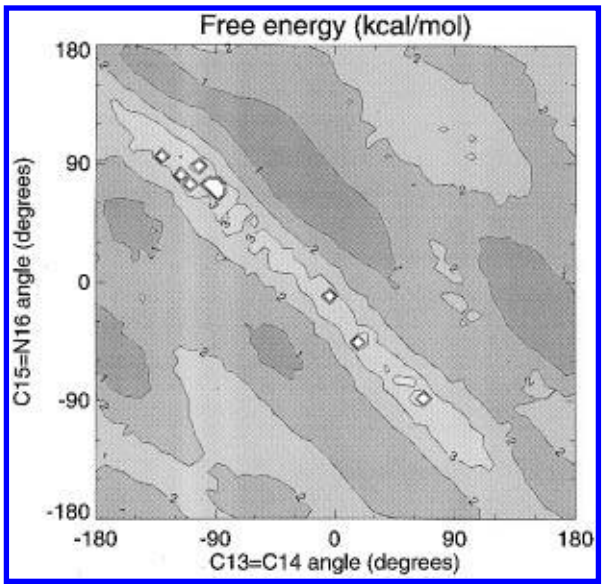

Figure 4. Free energy map for retinal computed from 16 ns free MD. The nonsampled regions are in white.

the *13cis,15trans* and *(13.15)cis* isomers, indicating that energy difference arises mainly from rotation around the C13═C14 bond.

The parametrization of the molecular mechanics energy function was made by comparing the molecular mechanical geometry-optimized energies with those obtained by *ab initio* for the four conformers. To reproduce the *ab initio* energies it was found to be necessary to modify the previously published molecular mechanics force field.[9] In particular, a too-strong van der Waals repulsion was found between carbon atoms C15 and C12 in the *trans* configuration. These sp^2 carbons are separated by three bonds (*i.e.*, they are vicinal, 1−4 atoms). To reduce the repulsion between them the van der Waals radius used for this 1−4 interaction was reduced and is given in Table 1. A further modification was of the intrinsic dihedral terms for the C13═C14 and C15═N16 angles. These are also given in Table 1 Set A. The energies of the geometry-optimized conformers obtained from the new molecular mechanics

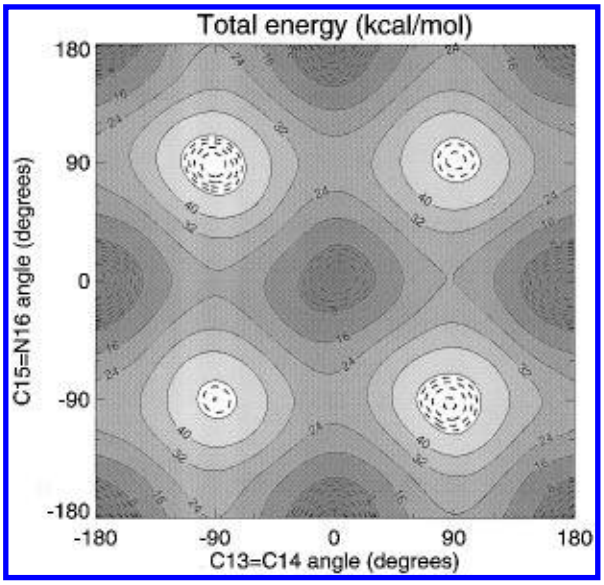

Figure 5. Adiabatic energy map computed with the full potential function of the retinal molecule (including Table 1 Set A).

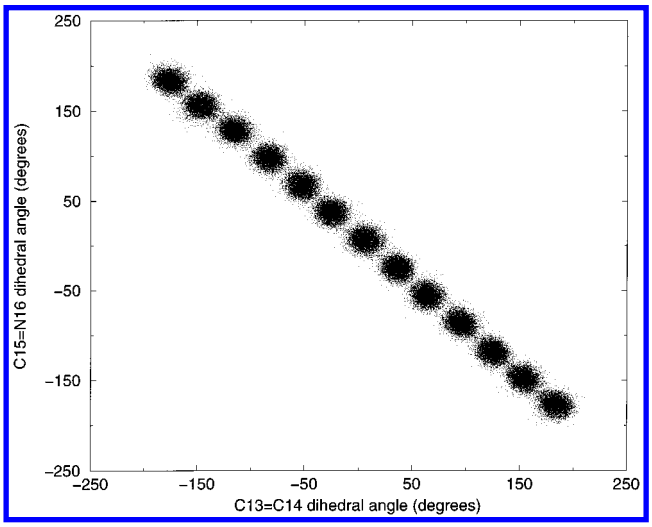

Figure 6. Dihedral angle distribution from umbrella sampling MD calculations with 250 ps/window.

force field are in good agreement with the *ab initio* results of Table 5(a).

Figure 3 shows the (ϕ_1, ϕ_1) adiabatic potential energy map, and Figure 4 shows the corresponding free energy map computed from the 16 ns free MD run. Some small parts of the free energy map are not sampled in the MD. Apart from these regions, the general forms of the free energy and adiabatic maps are similar. The "bicycle pedal" diagonal is not a minimum-energy pathway on these maps. However, as described in the Methods section, Figures 3 and 4 were calculated without the strong 2-fold torsional potential that represents the energy penalty for deforming the double bonds. When these are added, *i.e.*, with the potential of Table 1 Set A, the full potential map is obtained. Such a full potential adiabatic map, dominated by the 2-fold cosine function is shown in Figure 5. The *all-trans* ($\phi_1 = \phi_2 =$ 180°), *(13,15)cis* ($\phi_1 = \phi_2 = 0°$), *13-trans,15-cis,* and *13-cis,15-trans* structures are now all energy minima, with energies of 1.62, 4.07, 0.00, and 1.44 kcal/mol, respectively. The *13-trans,15-cis* and *13-cis,15-trans* conformations are of relatively low energy on Figure 5 but have not been observed in dark-adapted bR. This suggests that the protein

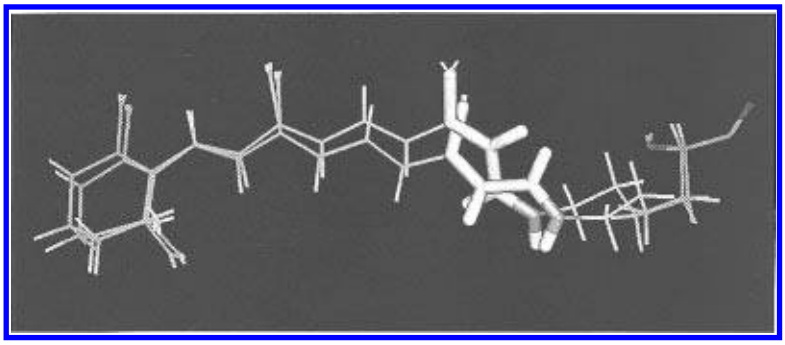

Figure 7. Superposition of *all-trans* and *(13,15)cis* retinal from the umbrella sampling calculations. The isomerized bonds are represented as cylinders.

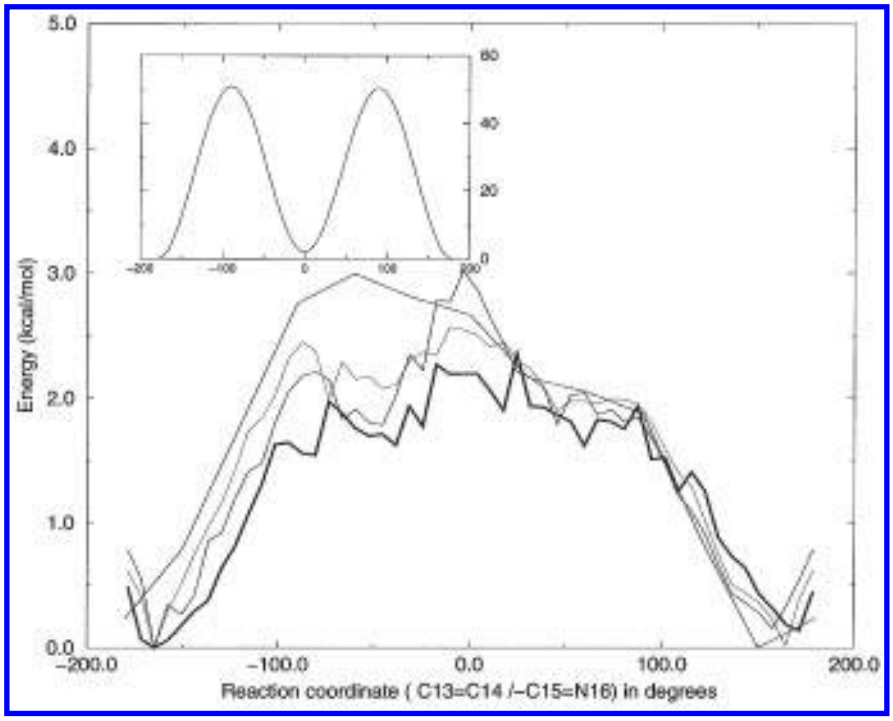

Figure 8. Energy profiles along the bicycle-pedal pathway. Blue: adiabatic potential energy. Black: 16 ns free MD free energy. Red: umbrella sampling free energy with 250 ps/window. Green: umbrella sampling free energy with 70 ps/window, except for windows centered at $\phi_1 = 120$, 90, -120, and $-90°$, for which 250 ps/window were run. The average difference between the green and black curves is 0.3 kcal/mol, with a standard deviation of 0.2 kcal/mol. INSET: free energy profile from the umbrella sampling simulation with 250 ps/window, calculated with the full potential function of the molecule, including the intrinsic dihedral terms of Table 1 Set A.

might have a destabilizing effect on them. Another effect of the protein should be to reduce the approximate 4-fold symmetry of the map in Figure 5, as the protein environment does not possess this symmetry. On Figure 5 the bicycle-pedal pathway again is not the lowest-energy isomerization pathway.

The WHAM method was used to calculate a free energy profile along the bicycle-pedal pathway. The dihedral angle distribution obtained in the umbrella sampling calculations is illustrated in Figure 6. In Figure 7 is shown a superposition of the average structures in the first and middle windows of the WHAM calculations, in which ϕ_1 and ϕ_2 are both *trans* and both *cis*, respectively. Whereas the overall shape of the retinal remains similar, some differences in the average positions of equivalent atoms are apparent, especially in the regions of the Schiff base.

Figure 8 compares the adiabatic energy profile along the bicycle-pedal pathway with free energy profiles calculated using the 16 ns free MD calculation and using WHAM with 250 ps/window (3.4 ns total simulation time). These profiles were calculated using the parameters of Table 1 Set B and do not include the 2-fold intrinsic C13═C14 and C15═N16 dihedral barriers of ~25 kcal/mol. However, as these intrinsic 2-fold barriers are zero at 0° and 180°, they do not change the *all-trans* − *(13,15)cis* energy difference of principal interest here. In the inset of Figure 8 is given the free energy profile along the bicycle pedal, calculated with the full parameter set Table 1 Set A, including the 2-fold intrinsic terms. The *all-trans* and *(13,15)cis* are minima of this profile.

The free energy profiles in Figure 8 are in an agreement with each other to within $\sim k_bT$ and give a free energy difference between the *(13,15)cis* and *all-trans* forms of retinal of $\sim 2.1 \pm 0.4$ kcal/mol. The adiabatic profile is similar to the PMF profiles, suggesting that the entropic contribution to the free energy difference is relatively small.

Finally, we examine the convergence properties of the free energy calculations. Tests indicated that an apparently-converged energy profile along the bicycle-pedal pathway was determined in 6 ns free MD; lengthening this to 16 ns produced only minor changes in the profile. The free MD/WHAM comparison confirms that the WHAM method can

produce similar results to free MD with a saving of computer time. Further calculations (not shown) suggest that using an even shorter sampling time of 180 ps/window (2.47 ns total) does not affect the WHAM results significantly. However, further reducing the time to 125 ps/window produces a free energy profile that differs significantly from the longer simulations by up to 1 kcal/mol. Finally, a calculation was performed with 70 ps/window for all windows except for those four for which the gradient of the potential of mean force is steepest—centered at $\phi^1 = 120°$, 90°, −120°, and −90°—for which the production time was set to 250 ps/window, giving a total simulation time of 1.72 ns. The potential of mean force thus calculated is also shown in Figure 8 and is still within $\sim k_bT$ of the other profiles.

CONCLUSIONS

The free energy calculations presented here all point to the *all-trans* conformation of retinal being more stable by $\sim 2.1 \pm 0.4$ kcal/mol in the present simulation model. The simulation model probes some of the effects on the populations of *all-trans* and *(13,15)cis* retinal in bR. The calculations were performed on retinal *in vacuo* with harmonic restraints designed such that the conformational flexibility of the *all-trans* chromophore in the protein is approximately reproduced. The calculations do not include explicit interactions between the protein and the retinal nor the effect of the retinal on the protein-protein interactions. As, in dark-adapted bR, the *(13,15)cis* and *all-trans* species are both significantly populated, with perhaps a higher proportion of the *(13,15)cis* conformation, the calculations presented here are consistent with an interpretation in which explicit protein: retinal interactions lead to a significant stabilization of the *(13,15)cis* form. Further calculations to examine these effects are in progress and will be reported later.

REFERENCES AND NOTES

(1) Oesterhelt, D. Stoeckenius, W. Rhodopsin-like protein from the purple membrane of *Halobacterium halobium. Nature (London), New Biol.* **1971**, *233*, 149−152.
(2) Henderson, R.; Baldwin, J. M.; Ceska, T. A.; Zemlin, F.; Beckmann, E.; Downing, K. H. Model for the structure of bacteriorhodopsin based on high-resolution electron cryo-microscopy. J. *Mol. Biol.* **l990**, *213*, 899−929.
(3) Grigorieff, T. A.; Ceska, K. H.; Downing, K. H.; Baldwin, J. M.; Henderson, R. Electron-crystallographic refinement of the structure of bacteriorhodopsin. *J. Mol. Biol.* **1996**, *259*, 393−421.
(4) Humphrey, W.; Logunov, I.; Schulten, K.; Sheves, M. Molecular dynamics study of bacteriorhodopsin and artificial pigments. *Biochemistry* **1994**, *33*, 3668−3678.
(5) Humphrey, W.; Xu, D.; Sheves, M.; Schulten, K. Molecular dynamics study of the early intermediates in the bacteriorhodopsin photocycle. J. *Phys. Chem.* **1995**, *99*, 14549−14560.
(6) Zhou, F.; Windemuth, A.; Schulten, K. Molecular dynamics study of the proton pump cycle of bacteriorhodopsin. *Biochemistry* **1993**, *32*(*9*), 2291−2306.
(7) Ferrand, M.; Zaccai, G.; Nina, M.; Smith, J. C.; Etchebest, C.; Roux, B. Structure and dynamics of bacteriorhodopsin: comparison of experiment and simulations. *FEBS Lett.* **1993**, *327*(*3*), 256−260.
(8) Nina, M.; Smith, J. C.; Roux, B. *Ab initio* quantum chemical analysis of retinal Schiff base hydration in bacteriorhodopsin. *J. Mol. Struct. (THEOCHEM)* **1993**, *286*, 231−245.
(9) Nina, M.; Roux, B.; Smith, J. C. Functional interactions in bacteriorhodopsin: a theoretical analysis of retinal hydrogen bonding with water. *Biophys. J.* **1995**, *68*, 25−39.
(10) Roux, B.; Nina. M.; Pomes. R.; Smith, J. C. Thermodynamic stability of water molecules in the bacteriorhodopsin proton channel: a molecular dynamics free energy perturbation study. *Biophys. J.* **1996**, *71*, 670−681.
(11) Harbison, G. S.; Smith, S. O.; Pardoen, J. A.; Winkel, C.; Lugtenburg, J.; Herzfeld, J.; Mathies, R.; Griffin, R. G. Dark-adapted bacteriorhodopsin contains 13-*cis*,15-*syn* and *all-trans*,*15-anti* retinal Schiff bases. *Proc. Natl. Acad. Sci. U.S.A.* **1984**, *81*, 1706−1709.
(12) Song, L.; Yang, D.; El-Sayed, M. A.; Lanyi, J. K. Retinal isomer composition in some bacteriorhodopsin mutants under light and dark adaptation conditions. *J. Phys. Chem.* **1995**, *99*, 10052−10055.
(13) Shulte, A.; Bradley II, L.; Williams, C. Equilibrium composition of retinal isomers in Dark-Adapted bacteriorhodopsin and effect of high pressure probed by near-infrared Raman spectroscopy. *Appl. Spectrosc.* **1995**, *49*, 80−83.
(14) Shulte, A.; Bradley II, L. High-pressure near-infrared Raman spectroscopy of bacteriorhodopsin light to dark adaptation. *Biophys. J.* **1995**, *69*, 1554−1562.
(15) Logunov, I.; Humphrey, W.; Schulten, K.; Sheves, M. Molecular dynamics study of the 13-*cis* form (bR_{548}) of bacteriorhodopsin and its photocycle. *Biophys. J.* **1995**, *68*, 1270−1282.
(16) Logunov, I.; Schulten, K. Quantum Chemistry: Molecular dynamics study of the dark-adaptation process in bacteriorhodopsin. *J. Am. Chem. Soc.* **1996**, *118*, 9727−9735.
(17) Humphrey, W. Personal communication.
(18) Kumar, S.; Bouzida, D.; Swendsen, R. H.; Kollman, P. A.; Rosenberg, J. M. The Weighted Histogram Analysis Method for free-energy calculations on biomolecules. I) The method. *J. Comput. Chem.* **1992**, *13*, 1011−1021.
(19) Roux, B. The calculation of the potential of mean force using computer simulations. *Comput. Phys. Commun.* **1995**, *91*, 275−282.
(20) Frish, M. J.; Head-Gordon, M.; Trucks, G. W.; Foresman, J. B.; Schlegel, H. B.; Raghavachari, K.; Robb, M.; Binkley, J. S.; Gonzales, C.; Defrees, D. J.; Fox, D. J.; Whitesick, R. A.; Seeger, R.; Melius, C. F.; Baker, J.; Martin, R. L.; Khan, L. R.; Stewart, J. J. P.; Topiol, S.; Pople, J. A. GAUSSIAN 90; Carnegie-Mellon University: Pittsburgh, PA.
(21) Brooks, B. R.; Bruccoleri, R. E.; Olafson, B. D.; States, D. J.; Swaminathan, S.; Karplus, M. CHARMM: a program for macromolecular energy minimization and dynamics calculations. *J. Comput. Chem.* **1983**, *4*, 187−217.
(22) Warshel, A. Bicycle-pedal model for the first step in the vision process. *Nature* **1976**, *260*, 679−683.
(23) Seltzer, S. MNDO barrier heights for catalyzed bicycle-pedal, hula-twist, and ordinary cis-trans isomerizations of protonated Schiff base. *J. Am. Chem. Soc.* **1987**, *109*, 1627−1631.

CI9702398